PROCEEDINGS OF SCIENCE

Recent ALICE results on photon-lead interactions

Roman Lavicka[a,*]

[a] *Stefan Meyer Institute for Subatomic Physics of the Austrian Academy of Sciences, Kegelgasse 27, 1030 Vienna, Austria*

E-mail: roman.lavicka@cern.ch

Photon-induced reactions in ultra-peripheral collisions (UPCs) of heavy nuclei at the LHC have been studied using the ALICE detector for several years. The ALICE detector can measure the photoproduction cross section for vector mesons at various rapidities, centre-of-mass energies and collision systems. In addition to the recent ALICE studies of the rapidity and momentum transfer dependence of coherent J/ψ photoproduction, new results on incoherent J/ψ photoproduction will be discussed. These results complement coherent J/ψ measurements and provide additional sensitivity to probing nuclear gluon effects.

HardProbes2023
26-31 March 2023
Aschaffenburg, Germany

*Speaker

PoS(HardProbes2023)059

1. Introduction

Photo-nuclear collisions can be studied in heavy-ion ultra-peripheral collisions (UPCs) at the LHC, where electromagnetic interactions dominate over hadronic interactions. An ultra-peripheral collision is defined as a collision where two projectiles pass each other with an impact parameter larger than the sum of their radii. Hadronic interactions are suppressed and electromagnetic interactions are manifested via photons with typically very small values of the momentum transfer squared Q^2. The physics of these processes is described in [1–3]. The intensity of the photon flux is growing with the nuclear charge squared and therefore lead-lead collisions provide large cross sections for the photo-production of vector mesons. Another advantage of this production is its clear experimental signature; the decay products are the only signal in otherwise empty detectors.

The differential vector meson cross section is

$$\frac{\mathrm{d}\sigma_{\mathrm{PbPb}}(y)}{\mathrm{d}y} = n_\gamma(y)\sigma_{\gamma\mathrm{Pb}}(y) + n_\gamma(-y)\sigma_{\gamma\mathrm{Pb}}(-y), \tag{1}$$

where $\mathrm{d}\sigma_{\mathrm{PbPb}}(y)/\mathrm{d}y$ is the cross section for a Pb–Pb collision, n_γ is the photon flux and $\sigma_{\gamma\mathrm{Pb}}$ is the photonuclear cross section. There are two possible contributions, each representing a different lead ion being the source of the photon. The relative weights of these contributions depend on rapidity (y). At midrapidity, both contributions are equal, but at forward rapidity the contributions differs. The energy of photon-nucleon system squared ($W^2_{\gamma\mathrm{Pb,n}}$) can be calculated as

$$W^2_{\gamma\mathrm{Pb,n}} = M_{\mathrm{J}/\psi}\sqrt{s_{\mathrm{NN}}}e^{\pm y}, \tag{2}$$

where $\sqrt{s_{\mathrm{NN}}}$ is the centre-of-mass energy per nucleon pair and $M_{\mathrm{J}/\psi}$ is the mass of J/ψ. Therefore at forward rapidity, each of the contributions is sensitive to gluons at different Bjorken-x ($x = M^2_{\mathrm{J}/\psi}/W^2_{\gamma\mathrm{Pb}}$). The high-$x$ contribution dominates [4], however if the low-x contribution is extracted, it allows us to test gluons at very low-x.

There are two types of diffractive vector meson photoproduction: Coherent, where the photon couples to the whole nucleus, and incoherent, where the photon interacts with single nucleons. While the coherent production is characterised by a low momentum ($p_{\mathrm{T}} \approx 60$ MeV/c), the incoherent one is more probable at higher momentum ($p_{\mathrm{T}} \approx 500$ MeV/c). In the first case, the nuclei usually do not break, but as the electromagnetic fields of lead nuclei are so strong, it is possible that there are other independent soft electromagnetic interactions which excite one or both of the nuclei. In the second case the nucleus breaks up and emits forward neutrons which can be measured in zero-degree calorimeters. The incoherent contribution can also be accompanied by the excitation and dissociation of the target nucleon resulting in even higher transverse momenta.

In these proceedings, results from two recent studies by the ALICE Collaboration are presented. One publication focus on measurements of the coherent J/ψ photonuclear production in Pb–Pb at $\sqrt{s_{\mathrm{NN}}} = 5.02$ TeV reconstructed via its muon decay channel [5]. In this analysis the events are classified according to the presence of accompanying neutrons at beam rapidities in order to disentangle the high- and low-energy contributions in Eq. (1). This measurement is then used to extract the photonuclear cross section, covering an unprecedentedly wide energy range. The other publication presents a measurement of incoherent J/ψ photonuclear production in Pb–Pb at $\sqrt{s_{\mathrm{NN}}} = 5.02$ TeV reconstructed via its muon decay channel, studying its dependency on the

momentum transfer $|t|$ [6]. This measurement is sensitive to subnucleonic structures of the gluon distribution in the nucleus.

2. Energy dependence of coherent J/ψ photonuclear production

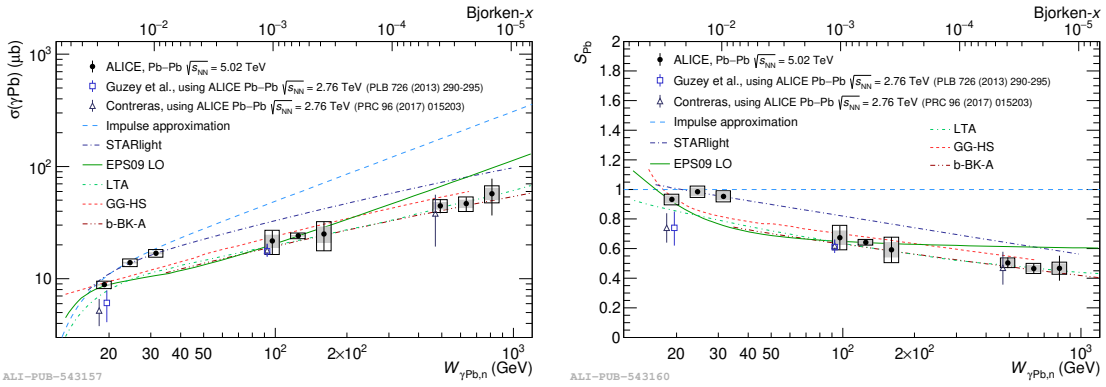

Figure 1: Photonuclear cross section for the $\gamma + \mathrm{Pb} \rightarrow \mathrm{J}/\psi + \mathrm{Pb}$ process (left) and nuclear suppresion factor calculated according to Eq. (3) (right); both as a function of $W_{\gamma \mathrm{Pb,n}}$ (lower axis) or Bjorken-x (upper axis). Various models [9–14] are compared to data. No model describes the measurement in full range. Taken from Ref. [5].

The measurement of the energy dependence of coherent J/ψ photonuclear production is reported as a function of the electromagnetic dissociation (EMD) of Pb [5]. The cross sections are presented in five rapidity intervals within $|y| < 4$. The EMD is accompanied by neutron production at beam rapidities, where these neutrons are detected by Zero Degree Calorimeters. The events are divided into four classes; one with no neutron activity (0n0n), two with activity in only one of the beam directions (0nXn or Xn0n) and one with activity in both directions (XnXn). As predicted in Ref. [7] and calculated in Ref. [8], the different neutron classes allow us to access different impact parameter and photon energy ranges. In view of Eq. (1) this means different photon fluxes n_γ, while the $\sigma_{\gamma \mathrm{Pb}}$ remains the same. Hence, measuring the left-hand side of Eq. (1) for different neutron classes allows us to disentangle the right-hand side cross sections and to estimate their values at different forward rapidities. This leads to a measurement of the photonuclear cross section in an unprecedentedly wide energy interval ($17 < W_{\gamma \mathrm{Pb,n}} < 920$) GeV, which corresponds to a Bjorken-x interval of $1.1 \times 10^{-5} < x < 3.3 \times 10^{-2}$. The results are shown and compared with models in Fig. 1, left panel.

The predictions obtained with the Impulse Approximation [9] and STARlight [10], the models which do not include gluon shadowing or saturation effects at all, are consistent with the data for the energy region below 40 GeV, but overestimate the measurements other energies. None of the other models EPS09-LO [11], LTA [12], b-BK-A [13], and GG-HS [14] models describe the data in the $W_{\gamma \mathrm{Pb,n}}$ range from about 25 to 35 GeV. The EPS09-LO and LTA models do not explicitly include gluon saturation, while the b-BK-A and GG-HS predictions do not include explicitly shadowing effects beyond saturation. The EPS09-LO model describes the measurements at the lowest energy and at intermediate energies, but overestimates the measurements at the highest energies. The GG-HS model does not include the reduction of phase space at low $W_{\gamma \mathrm{Pb,n}}$, but it describes the

data, except for the mentioned energy range, for all other measurements, with predictions which are systematically above the measurements. The predictions of the LTA and b-BK-A models are very similar and describe the data fairly well across these energies, except for the energy range from about 25 to 35 GeV. From the comparison to various models it can be concluded that the shadowing and saturation effects are not important at lower energies, while at higher energies gluon saturation and nuclear shadowing models describe well the data. More detail information on model comparisons can be found in Ref. [5].

The nuclear suppression factor is an interesting tool to quantitatively measure shadowing in this process as several theoretical uncertainties should largely cancel in the ratio. The nuclear suppression factor can be obtained by comparing to the Impulse Approximation model as in Eq. (3).

$$S_{\mathrm{Pb}} = \sqrt{\sigma_{\mathrm{data}}/\sigma_{\mathrm{IA}}} \tag{3}$$

The results are shown in Fig. 1, right panel. The nuclear suppression factor at low energies is about 0.94, decreases to values slightly above 0.64 at intermediate energies, and decreases further down to about 0.47 at the highest measured energies. The STARlight model describes only the $W_{\gamma\mathrm{Pb,n}}$ range from about 25 to 35 GeV. The other three models (EPS09-LO, LTA, GG-HS) do not describe this energy range, but provide a fair description at higher energies, except for the EPS09-LO model, which predicts a nuclear suppression factor that remains constant with increasing $W_{\gamma\mathrm{Pb,n}}$, while the data and the other models exhibit a decreasing trend. The predictions of LTA and b-BK-A are quite close to each other and follow the behaviour of data at all energies, except for the range from about 25 to 35 GeV, where b-BK-A prediction is missing.

3. $|t|$-dependence of incoherent J/ψ photonuclear production

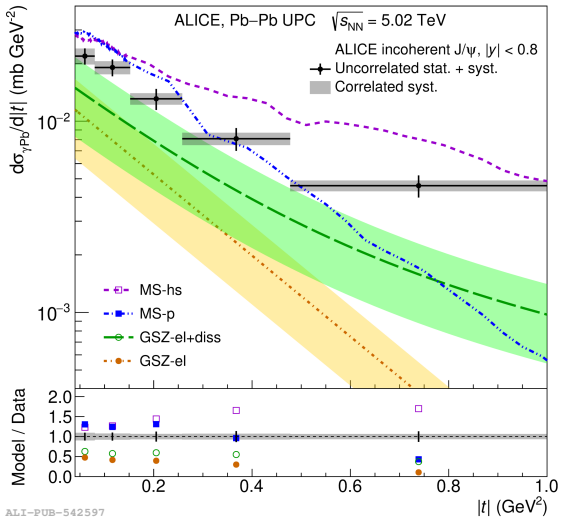

Figure 2: Cross section for the incoherent photoproduction of J/ψ vector mesons in ultra-peripheral Pb–Pb collisions at $\sqrt{s_{\mathrm{NN}}}$ = 5.02 TeV measured at midrapidity compared to different models [15, 16]. The bottom panel presents the ratio of the integral of the predicted to that of the measured cross section in each $|t|$ range. Taken from Ref. [6].

The measurement of the $|t|$-dependence of incoherent J/ψ photonuclear production, where $|t|$ is four-momentum transfer from the target nucleus squared (in this measurement $|t| \approx p_{\mathrm{T}}^2$ of the J/ψ), is reported in the rapidity interval $|y| < 0.8$, which corresponds to a Bjorken-x range of $(0.3 - 1.4) \times 10^{-3}$, and five $|t|$ intervals in the range $(0.04 - 1)$ GeV^2 [6]. The $|t|$-distribution is related to the nuclear/nucleon charge distribution through a Fourier transform. The incoherent production happens when a photon does not interact with the whole nucleus, but only with some of its constituents. Hence it is sensitive to its nucleon and sub-nucleon configuration and one expects $|t|$ to be in the range $(0.04 - 1)$ GeV^2.

There are two types of predictions. One including only the elastic interaction with single nucleons, and another where a dissociative-like component is included. The data are compared to work of two groups, each delivering both types of predictions. The model by Mäntysaari and Schenke (MS) [15] includes saturation and offers two predictions. In one, sub-nucleon fluctuations are not considered (MS-p), whereas in the other the proton is composed of three hot spots (MS-hs). The model by Guzey, Strikman, and Zhalov (GSZ) [16] expresses the incoherent cross section as the sum of an elastic and a dissociative part (GSZ-el+diss), both parameterised from HERA data, multiplied by a common factor representing shadowing. The inclusion of the dissociative component is interpreted by the authors within a Good–Walker approach as due to quantum fluctuations of the target. The prediction where the dissociative part is excluded (GSZ-el) is also presented.

The predictions are compared to the measurement in Fig. 2. The comparison has two characteristics. One is the normalisation, which is connected to the scaling from proton to nuclear targets, and the other is the slope, which refers to the size of the scattering object. None of the models describe both characteristics of data. Regarding the slope, it can be seen that the predictions which incorporates sub-nucleon degrees of freedom are less steep and agrees with the slope of data better, suggesting the importance of sub-nucleonic fluctuations at higher $|t|$.

4. Conclusion and outlook

The measurements of coherent and incoherent J/ψ photonuclear production as function of $W_{\gamma\mathrm{Pb,n}}$ (coherent production) and $|t|$(incoherent production) were presented. Various models were compared to data. Studying the energy distribution, it was found that at low energies weak gluon shadowing/no gluon saturation is visible. At higher energies, both effects can describe data well. Regarding the $|t|$-distribution, the sub-nucleonic degrees of freedom are important at higher $|t|$.

The ALICE detector has been upgraded [17] in order to handle the collection of new data which are being delivered in Run 3 and Run 4 [18]. These new data and new detector allow for reduction of systematic uncertainties and more detailed studies of UPCs.

References

[1] C. A. Bertulani, S. R. Klein and J. Nystrand, Ann. Rev. Nucl. Part. Sci. **55** (2005), 271-310 doi:10.1146/annurev.nucl.55.090704.151526 [arXiv:nucl-ex/0502005 [nucl-ex]].

[2] A. J. Baltz, G. Baur, D. d'Enterria, L. Frankfurt, F. Gelis, V. Guzey, K. Hencken, Y. Kharlov, M. Klasen and S. R. Klein, *et al.* Phys. Rept. **458** (2008), 1-171 doi:10.1016/j.physrep.2007.12.001 [arXiv:0706.3356 [nucl-ex]].

[3] J. G. Contreras and J. D. Tapia Takaki, Int. J. Mod. Phys. A **30** (2015), 1542012 doi:10.1142/S0217751X15420129

[4] M. Broz, J. G. Contreras and J. D. Tapia Takaki, Comput. Phys. Commun. **253** (2020), 107181 doi:10.1016/j.cpc.2020.107181 [arXiv:1908.08263 [nucl-th]].

[5] S. Acharya *et al.* [**ALICE** Collaboration], [arXiv:2305.19060 [nucl-ex]].

[6] S. Acharya *et al.* [**ALICE** Collaboration], [arXiv:2305.06169 [nucl-ex]].

[7] A. J. Baltz, S. R. Klein and J. Nystrand, Phys. Rev. Lett. **89** (2002), 012301 doi:10.1103/PhysRevLett.89.012301 [arXiv:nucl-th/0205031 [nucl-th]].

[8] V. Guzey, M. Strikman and M. Zhalov, Eur. Phys. J. C **74** (2014) no.7, 2942 doi:10.1140/epjc/s10052-014-2942-z [arXiv:1312.6486 [hep-ph]].

[9] G. F. Chew and G. C. Wick, Phys. Rev. **85** (1952) no.4, 636 doi:10.1103/PhysRev.85.636

[10] S. Klein and J. Nystrand, Phys. Rev. C **60** (1999), 014903 doi:10.1103/PhysRevC.60.014903 [arXiv:hep-ph/9902259 [hep-ph]].

[11] K. J. Eskola, H. Paukkunen and C. A. Salgado, JHEP **04** (2009), 065 doi:10.1088/1126-6708/2009/04/065 [arXiv:0902.4154 [hep-ph]].

[12] L. Frankfurt, V. Guzey and M. Strikman, Phys. Rept. **512** (2012), 255-393 doi:10.1016/j.physrep.2011.12.002 [arXiv:1106.2091 [hep-ph]].

[13] D. Bendova, J. Cepila, J. G. Contreras and M. Matas, Phys. Lett. B **817** (2021), 136306 doi:10.1016/j.physletb.2021.136306 [arXiv:2006.12980 [hep-ph]].

[14] J. Cepila, J. G. Contreras and M. Krelina, Phys. Rev. C **97** (2018) no.2, 024901 doi:10.1103/PhysRevC.97.024901 [arXiv:1711.01855 [hep-ph]].

[15] H. Mäntysaari and B. Schenke, Phys. Lett. B **772** (2017), 832-838 doi:10.1016/j.physletb.2017.07.063 [arXiv:1703.09256 [hep-ph]].

[16] V. Guzey, M. Strikman and M. Zhalov, Phys. Rev. C **99** (2019) no.1, 015201 doi:10.1103/PhysRevC.99.015201 [arXiv:1808.00740 [hep-ph]].

[17] S. Acharya *et al.* [**ALICE** Collaboration], [arXiv:2302.01238 [physics.ins-det]].

[18] Z. Citron, A. Dainese, J. F. Grosse-Oetringhaus, J. M. Jowett, Y. J. Lee, U. A. Wiedemann, M. Winn, A. Andronic, F. Bellini and E. Bruna, *et al.* CERN Yellow Rep. Monogr. **7** (2019), 1159-1410 doi:10.23731/CYRM-2019-007.1159 [arXiv:1812.06772 [hep-ph]].